

Article

Modeling and Simulation of Complex Fluid Networks in the Flue Gas System of a Boiler

Yue Zhang *, Yuhan Men and Pu Han

Department of Automation, North China Electric Power University, Yonghua North Street, No. 619, Baoding 071003, China; menyuhan@ncepu.edu.cn (Y.M.); hanpu102@263.net (P.H.)

* Correspondence: zdhzhangyue@ncepu.edu.cn; Tel.: +86-312-7522544

Received: 17 August 2017; Accepted: 13 September 2017; Published: 18 September 2017

Abstract: Under the conditions of high demand for energy saving and environmental protection, the thermal power unit is required to phase out the traditional extensive operation mode—a method of oxygen-enriched combustion in a furnace, considering safety first. Achieving efficient and economic operation with an optimal proportion of air distribution in these thermal power units is crucial. The high-precision simulation equipment could provide an experimental basis for optimal operation of field units. This paper starts by improving the accuracy of simulation equipment. In this work, the method of dividing nodes and branches in the boiler was based on signal flow graph theory. According to the flow characteristics of the working substance, the method for calculating the node and branch pressure drop was analyzed and set up. Subsequently, a fluid network model of the multi-dimensional flue gas system was constructed. With the help of our self-developed simulation model and data-driven platform, a modular simulation algorithm was designed. The simulation analysis of the boiler showed the accuracy of the model.

Keywords: thermal power plant; flue gas system; fluid network; nodes and branches; signal flow graph; simulation

1. Introduction

A decrease in electricity consumption has meant that the average utilization hours of thermal power units have decreased rapidly. Many thermal power units run at a low load for a long time, or the working conditions are adjusted frequently. Under severe environments, efficient and economic operation of the thermal power unit is important [1]. High-precision mathematical models can provide the necessary data support for operation optimization. The boiler equipment, especially the burning system, is a key component for achieving efficient operation optimization. An accurate description of the flow characteristics of a flue gas system has long-term significance. Many researchers have established many different types of flow-characterization models from different perspectives.

With the cold-flow model experiment, a cold test model was built to study gas flow characteristics in a boiler [2–4], potentially providing the basis for the design of a real boiler. Advanced measuring devices and methods were used to monitor the dynamic field of the boiler. The two-dimensional (2D) velocity field was reconstructed using the sound velocity distribution obtained by acoustic measurement [5]. An experimental investigation of the aerodynamic field in a four-cornered tangentially fired boiler was carried out using linear discriminant analysis (LDA) technology and a rotation method [6]. The powder velocity field in a boiler was set up using particle imaging velocimetry by dispersing tracer particles that followed the different motion of fluids in the two-phase particle flow field [7]. With the development of numerical simulation, the flow characteristics in a boiler could be simulated. Y. Zhou used the standard $k-\epsilon$ turbulence model to study the flow field of a tangentially fired boiler. The comparison error between the simulation result and test data was about

10% [8]. C.R. Choi and C.N. Kim conducted research on flow, burning and NO_x production in a tangentially fired boiler under different working conditions by using a re-normalization group (RNG) k - ϵ turbulence model [9]. J.T. Hart used standard k - ϵ , RNG k - ϵ and Reynolds stress models to simulate the aerodynamic field of the burner nozzle area in a tangentially fired boiler, and compared the errors of the three models [10]. N. Modlinski used a realizable k - ϵ turbulence model to study the effect of different swirl-plate angles on the flame temperature [11]. Even though numerical simulation techniques can describe dynamic and flow fields with high precision from microscopic images, further refinement of these models is needed.

The dynamic field of the fluegas in a boiler has the basic characteristics of a fluid network. Many studies have been conducted on the fluegas flow from a fluid network viewpoint. The use of a steady-state or quasi-steady-state model of a fluid network to analyze the dynamic characteristics of 1D or multi-dimensional fluid networks has developed rapidly. B. Ge built a network model of compressible fluid by analyzing the energy conservation and quality conservation of the nodes [12–14]. Considering the network similarity, an analog simulation method that could be applied to a general fluid network was proposed. The pressure model was analogous to a pure resistance linear circuit model, and the temperature model to a hypersurface model in L-dimensional Euclidean space [15,16]. K. Cai and other researchers analyzed two types of common fluid-network modeling methods: node pressure and network, and subsequently built a mathematic model of flow resistance of a fluegas system in a supercritical boiler [17].

To improve the accuracy of the node model, the pressure-correction method and integration have been combined to solve the problem of instability in fluid-network node modeling [18].

The network structure was established using graph theory, and the quasi-Newton iterative algorithm was used to calculate the transfer coefficient matrix [19]. The above fluid-network model could have described the flow characteristics macroscopically, but this was ignored in the report. The boiler was described as a node, and the model was inaccurate.

In recent years, advanced algorithms have been used in fluid network modeling. In 1998, W.H. Shayya and S.S. Sablani began to use artificial neural network models to calculate the friction coefficient along the fluid network [20]. The nonlinear fitting ability of the artificial neural network played an important role in modeling the complex fluid network. Furthermore, in 2012, S. Samadianfard introduced a genetic algorithm to calculate the hydraulic friction coefficient [21].

In recent years, with the ability to map a time series onto complex networks, progress has been made in complex multiphase nonlinear dynamics analysis. G. Zhongke et al. applied complex networks to the nonlinear analysis of multiphase flow, and pointed out that the two-phase flow conductivity time series based on experimental measurements could be used to construct complex networks [22]. Q. Sun et al. mapped the time series of the flow pressure difference onto complex networks. The identification of the air-water two-phase flow pattern and its nonlinear dynamic characteristics in a vertical riser was also studied by analyzing the community structure and statistical properties of the network [23]. To a certain extent, the complex network theory eradicates some of the shortcomings of simple networks.

This paper draws on the analysis theory of complex network structure to study the burning condition of the boiler. In this work, a fluid network model of a fluegas system in a tangentially fired boiler was constructed, based on the theory of a signal-flow diagram. The influence of gas-phase dynamic characteristics on the combustion process was described based on nodes and branches. As evidenced by specific examples, the model fully simulated the dynamic characteristics of the fluegas system in the boiler. It may also be applied in the simulator of thermal power units to provide model data for optimization and adjustment of combustion systems.

2. Fluid-Network Model Based on Signal Flow Graph Theory

Regardless of the type of internal working fluid, the fluid network is usually considered as nodes and branches connecting nodes in analysis and modeling.

In 1953, S.J. Mason proposed the signal flow graph that could be used to solve linear algebraic equations from topological graphs. The theory could be used for the analysis of feedback systems, solving linear equations, simulating linear systems and designing digital filters. The complex system was also described with nodes and directed segments with arrows [24]. With signal flow graph theory, nodes and branches can be used to describe the relationship of a device in a fluid network. However, the device not only corresponds to the nodes, but may also correspond to the branches. The connection between the devices may also correspond to both the nodes and branches.

The theory can be described as follows [25]:

- (1) When using the node to describe the device in a fluid network, it accurately reflects the change in pressure of the devices. The compressing process is neglected, such as the pumps and fans.
- (2) When using the node to describe the type of connecting pipeline among the devices, the pressure of the pipeline would change because it is under high pressure. The changing pressure could be calculated via the increasing number of nodes.
- (3) When using the branch to describe a connecting pipeline among the devices, it could reflect the change in mass and flow, and the change in pressure would be neglected.
- (4) When describing a device such as a valve, which mainly affects the change in mass and flow, the change in pressure could be obtained via node calculation.
- (5) There are three types of nodes in the signal flow graph: input, output and mixed nodes. During the setup of the model, the input and output nodes correspond to the boundary condition, which is usually atmosphere, or fluid with confirmed parameters, and so on.
- (6) The calculation of a mixed node is more complex. The impact from upstream and downstream of the node, and entering and out-flowing of the node, should be considered.

In this paper, the flow refers to mass flow. m_i is the mass of the fluid and q_{mi} is the flow of the branch passing through node i , which is defined where the flow entering the node is positive and that exiting is negative. $q_{m,ext}$ is the additional flow through node i , or the node characteristic correction. The magnitude of the positive and negative q_{mi} value is the same. V_i is the volume of node i , ρ_i is the density of the fluid, p_i is the pressure of node i and T_i is the temperature.

Thus, the mass conservation equation of a single node can be described as follows:

$$\frac{dm_i}{dt} = \sum q_{mi} + q_{m,ext}; \quad (1)$$

$$\frac{dm_i}{dt} = \frac{d(V_i \times \rho_i)}{dt} = V_i \left(\frac{\partial \rho_i}{\partial p_i} \times \frac{\partial p_i}{\partial t} + \frac{\partial \rho_i}{\partial T_i} \times \frac{\partial T_i}{\partial t} \right). \quad (2)$$

The length of the pipeline among the nodes and the node volume are constant. The density of the fluid varies with pressure and temperature, and the impact of the temperature is neglected. c_i denotes the change of density with pressure, or the compressive energy of the working fluids. For the uncompressed fluid, $d\rho_i/dp_i = 0$, and for the general fluid, the compressed coefficient is considered as a number close to zero. The relation between compressibility and flow is as follows:

$$\begin{aligned} c_i \frac{dp_i}{dt} &= \sum q_{mj} + q_{m,ext}; \\ c_i &= V_i \frac{d\rho_i}{dp_i}. \end{aligned} \quad (3)$$

The flow and pressure of the pipeline inlet is described by:

$$q_{mj} = C_m \cdot \sqrt{\Delta p}, \quad (4)$$

where C_m is the admittance of the pipeline, which reflects the circulation resistance, and Δp is the differential pressure of the pipeline inlet and outlet. The equation is nonlinear. The following is the result after Taylor series expansion, ignoring higher-order terms with an initial condition of zero:

$$\begin{aligned} q_{mj} &= q_{mj0} + \left. \frac{\partial q_{mj}}{\partial(\Delta p)} \right|_{q_{mj0}} (\Delta p - \Delta p_0); \\ q_{mj} &= B_m \cdot \Delta p; \text{ and} \\ B_m &= \left. \frac{C_m}{\sqrt{\Delta p}} \right|_0 = \left. \frac{\partial q_{mj}}{\partial(\Delta p)} \right|_{q_{mj0}}, \end{aligned} \quad (5)$$

where B_m is the admittance after linearization. Without considering the additional flow, the following results after linearization:

$$c_i \frac{dp_i}{dt} = \sum B_{sm} \Delta p_m - \sum B_{sn} \Delta p_n. \quad (6)$$

B_{sm} is the branch admittance that enters the node, and B_{sn} is the branch admittance that exits the node. p_j and q_{mi} are the upstream and downstream node pressure with a relationship of:

$$\begin{aligned} p_j > p_i > p_k \\ c_i \frac{dp_i}{dt} &= \sum B_{sm} (p_j - p_i) - \sum B_{sn} (p_i - p_k). \end{aligned} \quad (7)$$

p'_i is the final pressure, and Equation (7) can be described as:

$$c_i \frac{p_i - p'_i}{dt} = \sum B_{sm} (p_j - p_i) - \sum B_{sn} (p_i - p_k); \quad (8)$$

$$c_i \frac{p_i - p'_i}{dt} = \sum B_{sm} p_j - \sum B_{sm} p_i - \sum B_{sn} p_i + \sum B_{sn} p_k; \text{ and} \quad (9)$$

$$c_i \frac{p_i}{dt} + \sum B_{sm} p_i + \sum B_{sn} p_i = c_i \frac{p'_i}{dt} + \sum B_{sm} p_j + \sum B_{sn} p_k. \quad (10)$$

Subsequently, the formula of node pressure p_i can be obtained:

$$p_i = \frac{c_i \frac{p'_i}{dt} + \sum B_{sm} p_j + \sum B_{sn} p_k}{\frac{c_i}{dt} + \sum B_{sm} + \sum B_{sn}}. \quad (11)$$

After Laplace variation of Equation (7) under an initial condition of zero:

$$P_i(s) = \frac{\sum B_{sm} P_j(s) + \sum B_{sn} P_k(s)}{c_i S + \sum B_{sm} + \sum B_{sn}}. \quad (12)$$

p_i is determined by the pressure of the final moment, and the upstream and downstream pressure. The equivalent transfer coefficient form among the nodes is the first-order inertia element.

3. Model of the Single-Layer Tangentially Fired Boiler

The nozzle form of the tangential burner was a rectangular jet. The overall pressure drop included that of the primary airduct and that of the jet from burner to boiler. The flow resistance coefficient of the equivalent branch was obtained using the total pressure drop and the mass flow [26].

3.1. Pressure Drop of the Primary Airduct

In the primary airduct, the mixture of primary air and pulverized coal was a typical dilute gas–solid flow. There were two types of pressure drop: the working fluid acceleration pressure drop, and the frictional pressure drop. The latter was composed of two drops corresponding to the gas and solid phase.

The acceleration pressure drop can be described as:

$$\Delta p_{acc} = \frac{\rho_g v_g^2}{2} \left(1 + \mu \left(\frac{v_s}{v_g}\right)^2\right), \quad (13)$$

where μ is the powder concentration, ρ_g is the gas density, v_g is the gas velocity and v_s is the solid velocity.

The friction pressure drop is given by:

$$\Delta p_f = \Delta p_{fg} + \Delta p_{fs} = \lambda_g \frac{L \rho_g v_g^2}{d} + \mu \frac{v_s}{v_g} \lambda_s \frac{L \rho_g v_s^2}{d} = \lambda_g \frac{L \rho_g v_g^2}{d} \left(1 + \mu \frac{\lambda_s v_s}{\lambda_g v_g}\right), \quad (14)$$

where λ_g is the equivalent friction coefficient of the gas phase, λ_s is the equivalent friction coefficient of the solid phase, L is the length of the pipeline and d is the diameter of the pipeline.

3.2. Pressure Drop in Boiler

The nozzle form of the tangential burner was a rectangular jet. The pressure drop of the jet from burner to boiler could be calculated with jet speed along the direction of the nozzle.

The expanding angle of the jet can be calculated using:

$$\cot \frac{\theta}{2} = \frac{x_0}{b_0} = \frac{0.41}{a}, \quad (15)$$

where x_0 is the distance from the jet origin to the nozzle, and b_0 is the nozzle radius.

The relation between the two is as follows:

$$\frac{\omega_m}{\omega_0} = \frac{1.2}{\sqrt{a \frac{x}{b_0} + 0.41}}; \text{ and} \quad (16)$$

$$\frac{\omega_x}{\omega_m} = \left[1 - \left(\frac{y}{y_{bj}}\right)^{\frac{2}{3}}\right]^2, \quad (17)$$

where a is the empirical constant (related to the turbulence degree of the airflow and the uniform distribution of the velocity field at the nozzle), ω_0 is the initial speed of the nozzle and x is the distance measured to the nozzle. ω_m is the speed at axis x from the nozzle, and ω_x is the speed at axis x from the nozzle. y is the distance to the axis, and y_{bj} is the distance between the axis and the boundary.

The pressure drop is calculated based on the change in the jet velocity:

$$\Delta p_{acc} = (1 + c_0) \frac{\rho(\omega_0^2 - \omega_m^2)}{2}, \quad (18)$$

where c_0 is the density of coal fines.

3.3. Tangential Boiler Model of Single-Layer with FourCorners

The signal flow graph model of the single-layer tangentially fired boiler was built as shown in Figure 1. S_i is the node of pressure, and i is from 0 to 8. S_0 is the inlet pressure node of the air–powder pipe. S_j is the outlet pressure node of the air–powder pipe, and j is from 1 to 4. S_k is the pressure node of the injector, and k ranges from 5 to 8. S_k reflects the position and pressure of the circle.

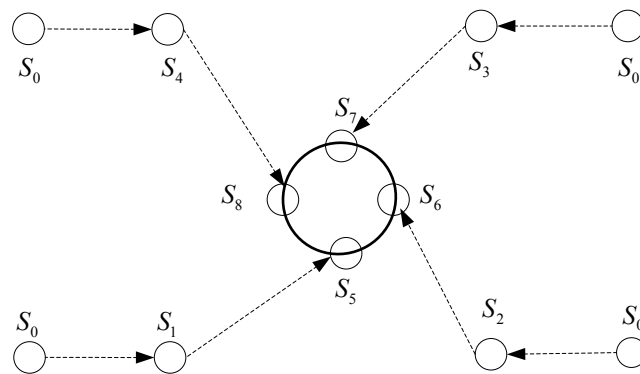


Figure 1. Model of the single-layer tangentially fired boiler.

Table 1 shows the structure and parameters of the 350 MW supercritical coal-fired units. Figure 2 is the hypothetical tangential structure for theoretical calculation.

Table 1. Parameters of the boiler structure.

Parameter	Value	Parameter	Value	Parameter	Value
Width of boiler	14.904 m	Length of boiler	14.094 m	Height of boiler	61.900 m
Number of burner layers	5	Number of secondary air layers	6	Number of over-fire air layers	2
Elevation of the top burner	27.402 m	Elevation of the lowest burner	20.566 m		
Internal diameter of pulverized coal nozzle	0.51 m	External diameter of pulverized coal nozzle	0.53 m		

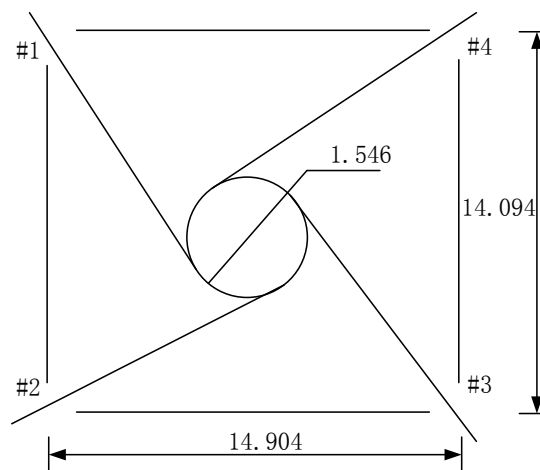


Figure 2. Hypothetical tangential structure for theoretical calculation.

On the simulation platform STS (Simulation Training System), which was designed independently, algorithms were designed to calculate the node pressure, the pressure drop of the air-powder pipeline and the jet flow. Figure 3 shows the module distribution and connection relationship in STS.

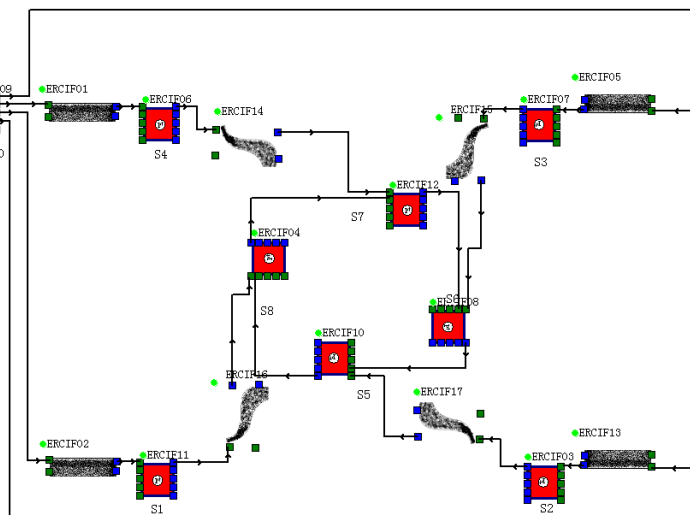


Figure 3. Simulation model of the single-layer tangentially fired boiler.

On the simulation platform, the response curves of key parameters with different inputs and external disturbance were studied, as shown in Figure 4.

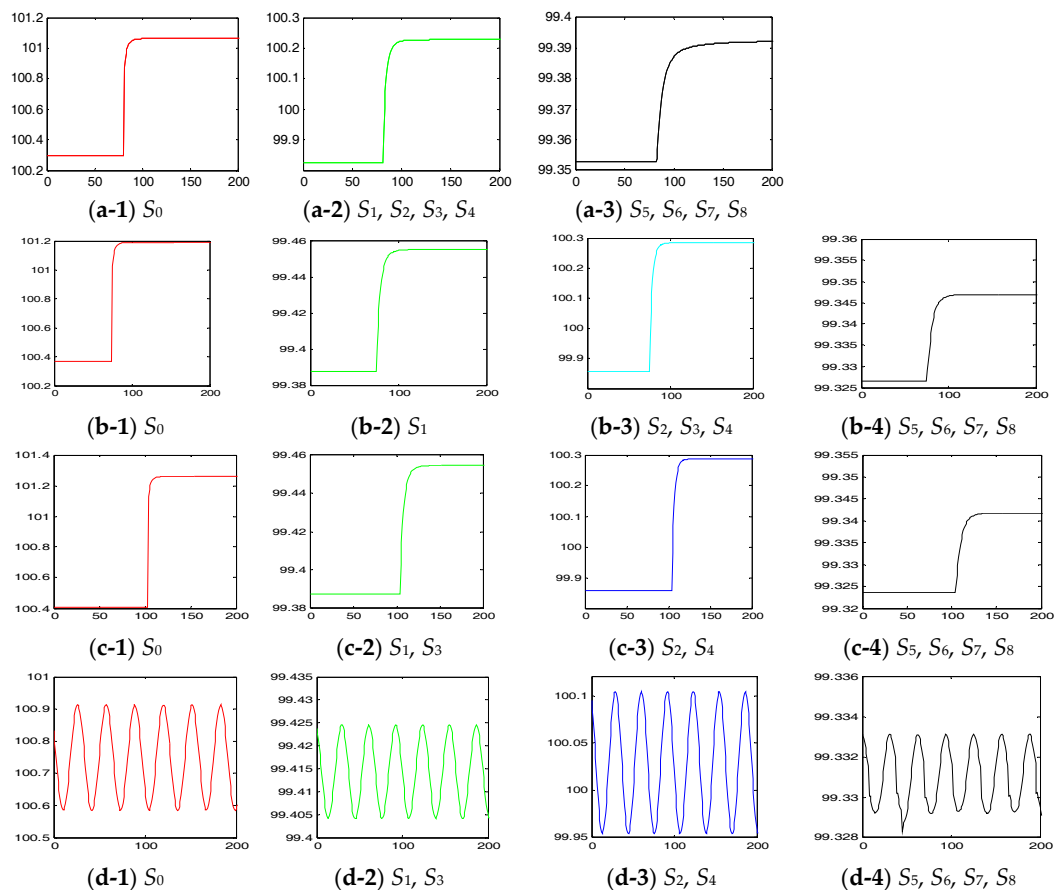


Figure 4. Response curves of the (a) powder entrance with pressure disturbance; (b) powder entrance with pressure disturbance when powder pipe 1 was blocked; (c) powder entrance with pressure disturbance when powder pipes 1 and 3 were blocked; and (d) powder exit with pressure disturbance when powder pipes 1 and 3 were blocked.

In the subfigures, the ordinate is absolute pressure and the unit is KPa. By changing the inlet pressure disturbance of the air-powder pipe, the response curves of the air-powder pipe outlet pressure and the injector pressure were studied.

It can be seen from the subfigures that the position and pressure of the tangential circle varied with the pressure of the separator outlet of the coal grinding machine (and the inlet of the air-powder pipeline). When the air-powder pipelines were blocked, the amplitude of the pressure varied. According to the curve in Figure 4d, on the same branch of the fluid network, the pressure change of the downstream node lagged behind the front node. The lag time was adjusted by c_i in the node calculation process.

4. Tangential Boiler Model of the Direct-Current Burner with Intersecting Adjacent Multilayers

Figure 5 shows the position of the primary and secondary air pipelines in the single layer of the 350 MW boiler. The nodes of the signal flow graph are shown in Figure 6.

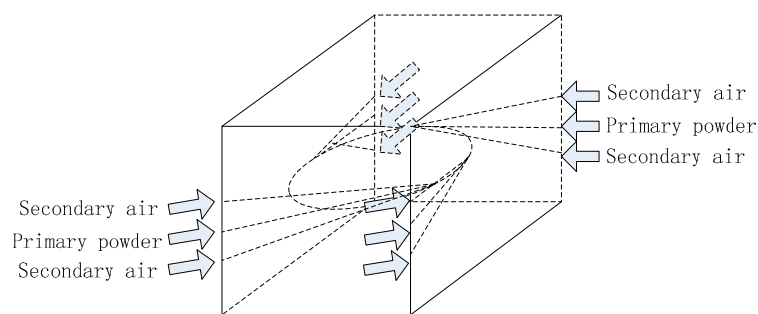


Figure 5. Burners in the single layer and positions of the air ducts in the boiler.

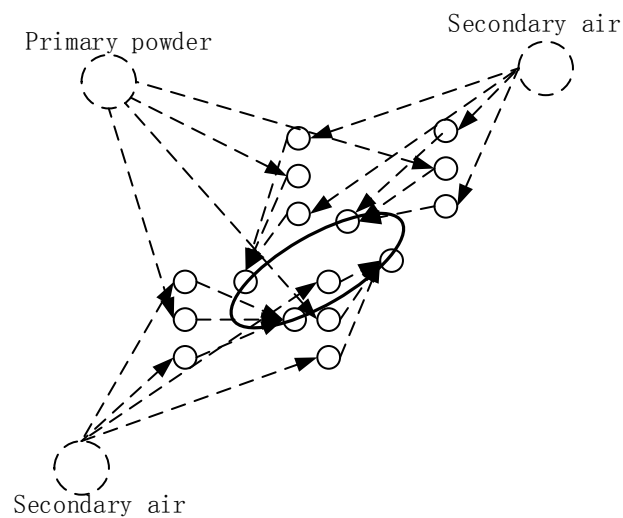


Figure 6. Burners of the single layer and model of the signal flow graph of the boiler.

The calculation of the pressure drop in the secondary airduct was relatively simple compared to the calculation of the pressure drop in the air-powder duct. This pressure drop was composed of the acceleration and friction pressure drops.

These pressure drops were calculated for the fluid in a single phase by:

$$\Delta p_{acc} = \zeta \frac{\rho_g v_g^2}{2}, \quad (19)$$

where ζ is the equivalent resistance coefficient. Considering the influence of secondary air, the result is shown in Figure 7.

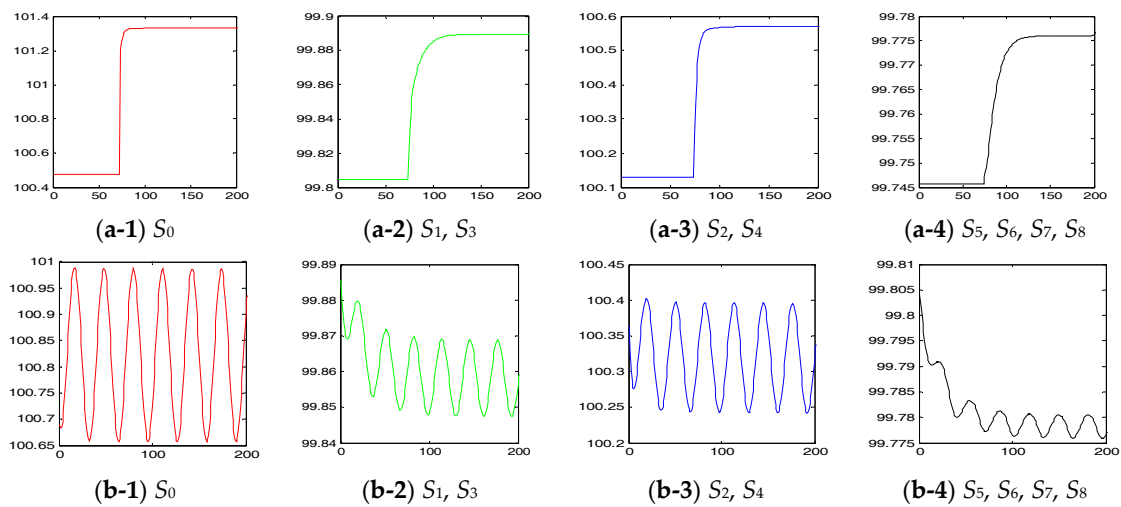


Figure 7. Response curves of the (a) powder entrance with pressure disturbance when powder pipes 1 and 3 were blocked, and (b) powder exit with pressure disturbance when powder pipes 1 and 3 were blocked, under the influence of secondary air.

Compared with the simulation result in Figure 4, the influence of the outlet pressure of the coal-grinding machine on the pressure position of the tangential circle reduced. In the figures, the ordinate is also absolute pressure, and the unit is KPa. By changing the inlet pressure disturbance of the air-powder pipe, the curves of the air-powder pipe outlet pressure and the injector pressure were studied.

5. Overall Network Model and Simulation Verification

5.1. Overall Network Model

There were 5 pulverizing systems in the 350 MW supercritical units. The nodes are shown in Figure 8.

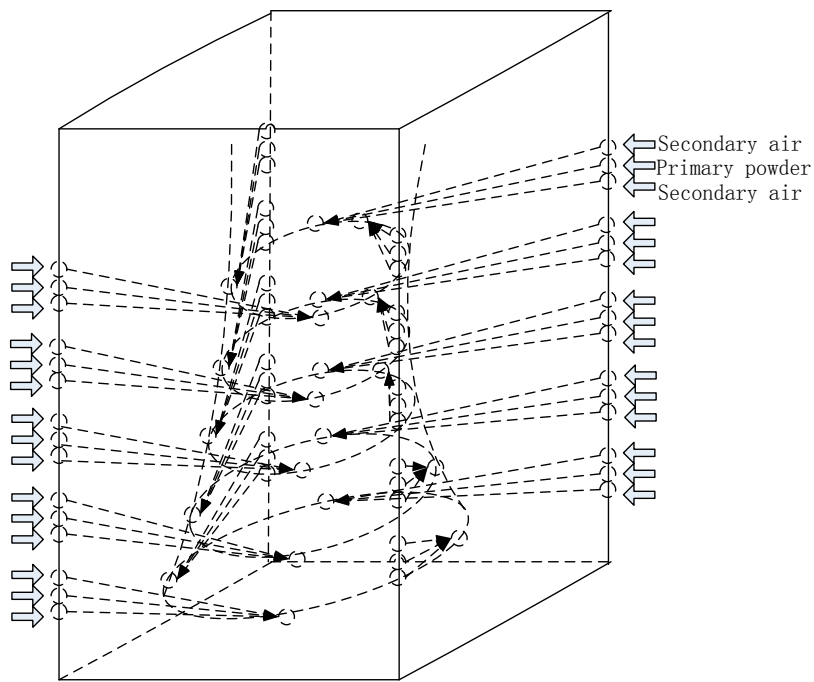


Figure 8. Node distribution of the air–gas fluid network in the boiler.

5.2. Simulation of the Overall Dynamic Model

The simulation curves under different inputs and disturbances are shown in Figure 9.

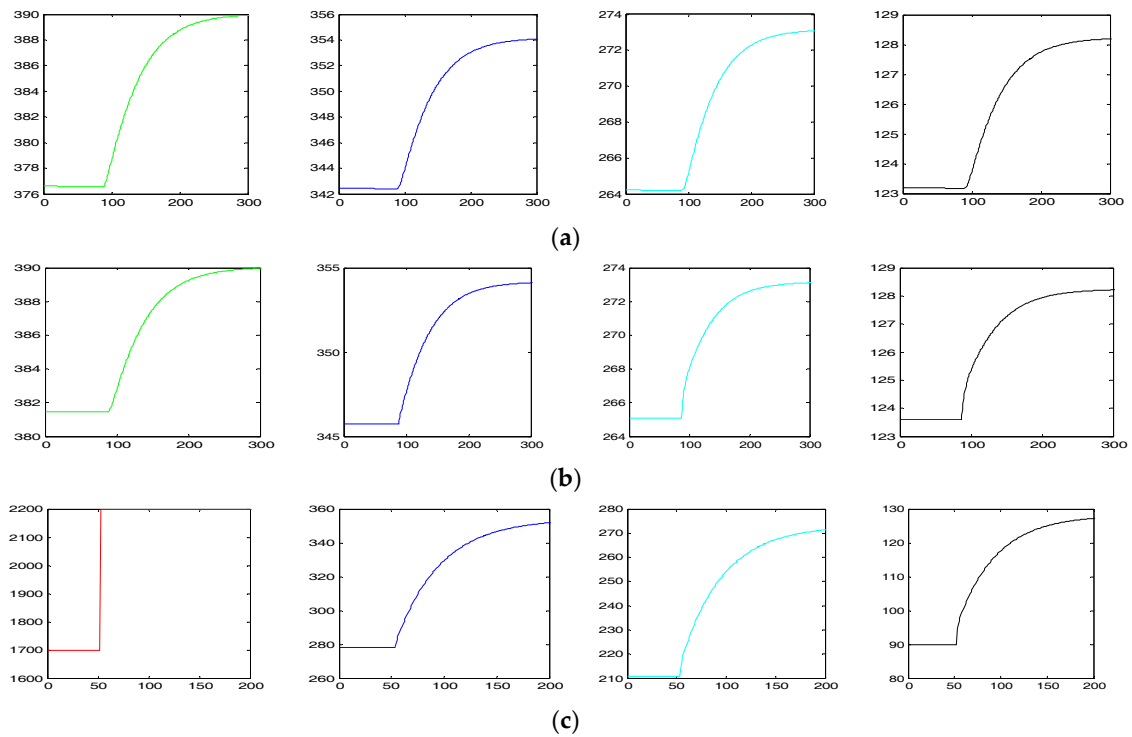


Figure 9. Cont.

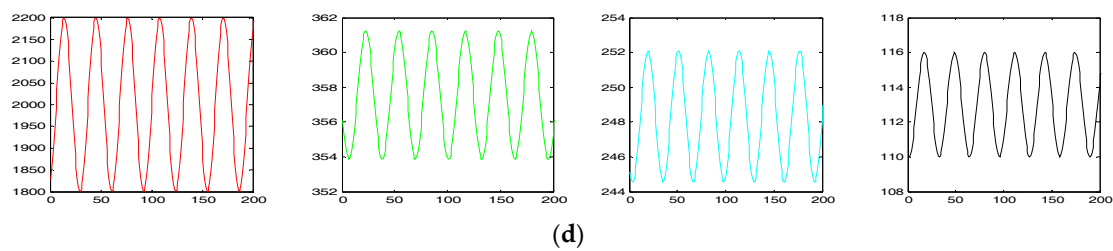


Figure 9. Tangential circle pressure at different heights (a) under the outlet pressure fluctuation of the bottom separator; (b) under the outlet pressure fluctuation of the middle separator; and (c) under pressure fluctuation of secondary air. (d) Tangential circle pressure changing condition at different heights under pressure fluctuation of secondary air.

In the subfigures, the ordinate is gauge pressure and the unit is Pa. The tangential circle pressure at different heights was studied. On comparing the simulation curves, it is evident that the influence of the outlet pressure fluctuation of the bottom separator on the tangential circle pressure was greater than that of the middle separator. The influence of the pressure fluctuation of secondary air on the tangential circle pressure was greater than that of the primary air.

6. Conclusions

By analyzing the characteristics of a mixture of wind and powder, a complex multi-dimensional fluid network model was built to describe the change in node pressure in the boiler under different ratios of wind to powder. Thus, the flow characteristics of the complex fluid in the boiler were obtained.

It is hoped that the research results will improve the accuracy of thermal-power-unit simulations and can be used for further research about optimal operation. The modeling method and process were described with the help of our self-developed simulation platform (STS). The simulation results showed that the model obtained can demonstrate the characteristics of the fluid network in a boiler.

Acknowledgments: The work described in this paper was fully supported by the Central Universities Fundamental Research Fund under Grant (9160315006).

Author Contributions: Yue Zhang did the simulations, data analysis and wrote part of this paper. Yuhan Men provided the original idea and wrote part of this paper. Pu Han did the data analysis.

Conflicts of Interest: The authors declare no conflict of interest.

References

1. Zeng, M.; Zhang, X.; Zhang, P.; Dong, J. Overall review of China's thermal power development with emphatic analysis on thermal powers' cost and benefit. *Renew. Sustain. Energy Rev.* **2016**, *63*, 152–157.
2. Chang, S.; Wu, W.; Huang, J.; Li, B. Turbulence model of aerodynamic field in cold experimental model for tangential fired boiler. *Therm. Power Gener.* **2013**, *2*, 62–66.
3. Zhang, H.J.; Gao, Z.Q.; Zhao, K.; Tao, M.; Hui, S.E.; Zhou, Q. Study of aerodynamic characteristics of concentric system in tangential firing boiler. *Power Eng.* **2004**, *4*, 481–484.
4. Liu, Y.; Wei, F.; Tang, B.G. Experimental research on flue gas flow characteristics of foursquare tangential circle boiler in cold aerodynamical field. *Eng. J. Wuhan Univ.* **2002**, *35*, 52–55.
5. Li, Y.Q.; Zhou, H.C. Simulation study on complicated 2-D aerodynamic field in boiler furnaces for acoustic monitoring purposes. *Power Eng.* **2004**, *6*, 836–839.
6. You, C.; Qi, H.; Xu, X.; Baudoin, B. Experimental investigation on gas flow in a model of tangentially-fired boiler. *J. Eng. Thermophys.* **2001**, *3*, 386–389.
7. Dong, K.; Zhou, H.; Yang, Y.; Wang, L.L.; Cen, K.F. Influence of mass flow rate of secondary air on gas/solid flow characteristics of a swirl burner. *J. Zhejiang Univ. (Eng. Sci.)* **2014**, *12*, 2162–2171.
8. Zhou, Y.; Xu, T.; Hui, S.; Zhang, M. Experimental and numerical study on the flow fields in upper furnace for large scale tangentially fired boilers. *Appl. Therm. Eng.* **2009**, *4*, 732–739. [[CrossRef](#)]

9. Choi, C.R.; Kim, C.N. Numerical investigation on the flow, combustion and NO_x emission characteristics in a 500 MWe tangentially fired pulverized-coal boiler. *Fuel* **2009**, *9*, 1720–1731. [[CrossRef](#)]
10. Hart, J.T.; Naser, J.A.; Witt, P.J. Aerodynamics of an isolated slot-burner from a tangentially-fired boiler. *Appl. Math. Model.* **2009**, *9*, 3756–3767. [[CrossRef](#)]
11. Modlinski, N. Computational modeling of a utility boiler tangentially-fired furnace retrofitted with swirl burners. *Fuel Process. Technol.* **2010**, *11*, 1601–1608. [[CrossRef](#)]
12. Ge, B. Application of compressible fluid flow network in real time simulation of power plants. *Power Eng.* **2002**, *6*, 2119–2122.
13. Zhang, Y.; Han, P.; Chen, W. Modelling on air-flue gas system of fluidized-bed boilers based on signal flow graphs. *J. Chin. Soc. Power Eng.* **2014**, *7*, 524–528.
14. Cai, R.; Zhang, L.; Xie, M.Q.; Zhu, W.; Li, T. Real-time simulation model and algorithm for thermo hydraulic network. *J. Syst. Simul.* **1992**, *4*, 13–18.
15. Song, D.H.; Li, S.H. The exploration of applying the fluid network theory to solve the fluid network model of thermodynamic system. *Turbine Technol.* **2016**, *2*, 95–97.
16. Shi, X.P.; San, Y. A Sort of analogical modeling method of liquid networks. *J. Syst. Simul.* **2001**, *1*, 34–36.
17. Cai, K.; Chen, Q.J.; Wang, J.M.; Hu, N.-S. Dynamic mathematical model for fluid network of air and flue gas system of supercritical boilers. *J. Power Eng.* **2009**, *2*, 134–138.
18. Hou, S.P.; Tao, Z.; Han, S.J.; Ding, S.T.; Xu, G.-Q.; Wu, H. New simulation approach to the unsteady fluid network and the application. *J. Aerosp. Power* **2009**, *6*, 1253–1257.
19. Liao, J.J.; Zou, X.X.; Li, B.-R. Study on variable flow resistance method for analysis on fluid system network. *Ship Sci. Technol.* **2013**, *4*, 40–44.
20. Shayya, W.H.; Sablani, S.S. An artificial neural network for non-iterative calculate of the friction factor in pipeline flow. *Comput. Electron. Agric.* **1998**, *3*, 219–228. [[CrossRef](#)]
21. Samadianfard, S. Gene expression programming analysis of implicit Colebrook-White equation in turbulent flow friction factor calculation. *J. Pet. Sci. Eng.* **2012**, *92*, 48–55. [[CrossRef](#)]
22. Gao, Z.K.; Jin, N.D.; Wang, W.X.; Lai, Y.C. Motif distributions in phase-space networks for characterizing experimental two phase flow patterns with chaotic features. *Phys. Rev. E-Stat. Nonlinear Soft Matter Phys.* **2010**, *1*, 016210. [[CrossRef](#)] [[PubMed](#)]
23. Sun, Q.M.; Zhang, B.; Zhang, H. Flow pattern identification and dynamics characteristics analyses for gas-liquid two-phase flow in complex network. *J. Dalian Univ. Technol.* **2015**, *5*, 470–477.
24. Mason, S.J. Feedback Theory-Further Properties of Signal Flow Graphs. *Proc. IRE* **1956**, *44*, 920–926. [[CrossRef](#)]
25. Zhang, Y.; Han, P. A Fluid network modeling method based on the theory of signal flow graph. *J. Syst. Simul.* **2016**, *5*, 1038–1044.
26. Zhao, M.; Huang, K.; Wang, H.; Shen, Y.Y.; Yang, M. Numerical simulation of asymmetrical cold flow in a boiler furnace with four corners tangential firing structure. *J. Eng. Thermophys.* **2014**, *5*, 952–955.

